Journal of
Nanoscience and Nanotechnology
Vol. 10, 3934–3939, 2010

Doping of Carbon Nanotubes Using Low Energy Ion Implantation

Jin Ho Jang[1, †], Seong Chu Lim[2, †], Dihn Loc Duong[1], Gunn Kim[1], Woo Jong Yu[3], Kang Hee Han[1], Yo-Sep Min[4, ‡], and Young Hee Lee[1, 2, 3, *]

[1] *BK21 Physics Division,* [2] *Center for Nanotubes and Nanostructured Composites,*
[3] *Sungkyunkwan Advanced Institute of Nanotechnology,*
Sungkyunkwan University, Suwon 440-746, Republic of Korea
[4] *Department of Chemical Engineering, Konkuk University, Seoul 143-701, Korea*

Carbon nanotubes (CNTs) were implanted with thermally decomposed oxygen (O_2^+) and nitrogen (N_2^+) ions at an acceleration voltage of 20 V. With a low dose of oxygen ions, the CNT-FET exhibited *p*-type behaviors with substantial changes in threshold voltage and in the slope of the source–drain current (I_{sd}). However, at high dosages, the device exhibited metallic behaviors. After nitrogen doping, we did not observe the effects of electron doping. Instead, nitrogen doping significantly increased I_{sd} with no gating effect. Our theoretical results showed that the metallic behavior of nitrogen-doped CNTs arose from the impurity conduction band, which results from the overlapping wave function of the nitrogen impurity.

Keywords: Carbon Nanotubes, Doping, Ion Implantation, Oxygen, Nitrogen.

1. INTRODUCTION

Continuously improving device performance in the silicon industry has been largely achieved by downsizing device dimensions. However, this approach will soon meet scientific and technical limitations. CNTs are attractive as a solution to the forthcoming fabrication barrier. They are about 1 nm in diameter, a few micrometers in length, and are attractive semiconducting materials with a band gap of 0.5–1.0 eV, high mobility and large current carrying capability, and a direct band gap.[1–4]

However, CNTs have shown *p*-type behavior in air due to the adsorption of oxygen onto the metal-CNT junction.[5] In addition, although the implantation of electron carriers into the CNT-FET is essential to fabricating complementary metal-oxide semiconductor (CMOS) circuits, it has been achieved only with certain approaches, such as the use of alkali metals, polymers, and low work function metals like Ca.[6–8] Some doping techniques have been adapted to enhance the electrical conductivity of CNT networks.[9, 10] However, these techniques raise issues of stability and processability. For instance, potassium may not sustain in the chemicals used for micro-processes and air operation.[6] In addition, control of the doping concentration is not feasible in some methods.[8]

Ion implantation is used for Si devices, since it allows a precise control of carrier concentration and doping area. However, the use of ion beams in the MeV range may not be suitable for nanostructures like CNTs. Therefore, we used a low acceleration voltage of around 20 V with Ar, O_2, and N_2 gases. These gases were decomposed using a W hot filament and then accelerated toward the CNTs. The degree of doping was monitored *in-situ* with gas pressure, ion current, and exposure time.

We observed that at low doping concentrations, oxygen contributed to *p*-type behavior of the CNT-FET, whereas at high doping concentrations, it gave rise to metallic behavior. Under nitrogen irradiation, on the other hand, no distinctive *n*-type characteristics were observed at low ion dosages, whereas at high ion dosages strong metallic characteristics were seen with a significant increase in the source–drain current (I_{ds}) of five orders of magnitude. Our calculations suggest that such a large increase in I_{ds} was presumably caused by the formation of metallic channels through the impurity conduction band.

2. EXPERIMENTAL DETAILS

We grew CNTs using water-plasma chemical vapor deposition (CVD).[11] For selective growth between the

*Author to whom correspondence should be addressed.
†These authors contributed equally to this work.
‡Present address: FPRD and Department of Physics and Astronomy, Seoul National University, Seoul 151-747, Korea.

1533-4880/2010/10/3934/006 doi:10.1166/jnn.2010.1989

source–drain electrodes, catalyst particles were mixed with e-beam resist, spin coated on Si substrate, and selectively removed using e-beam lithography. The oxide thickness on the Si substrate was about 500 nm. The CVD-grown CNTs were mostly single-walled with a diameter of 2–3 nm. Ti/Au electrodes were deposited onto the CNTs using a thermal evaporator. Prior to doping, the *I–V* characteristics of each CNT-FET were examined in air and then in a vacuum system at a base pressure of about 1×10^{-7} torr. Electrical feedthroughs allowed us to monitor the effect of *in-situ* doping. Before exposing the CNTs to energetic ions, degassing of the sample was performed using a W filament. A filament temperature of about 3000 °C was measured using an optical pyrometer. Radiation from the W filament caused the substrate temperature to increase to approximately 150–200 °C for the 30 minute degassing process. After releasing the gas adsorbates from the CNT-FET, I_{ds} was measured at room temperature using Keithley 236 and 237 source-measure units.

Argon, oxygen, and nitrogen gases with purities of 99.999% were introduced into the chamber for doping, then thermally cracked using a W filament, and accelerated under 20 volts between the W filament and the substrate. During the process, the chamber pressure was 4.0×10^{-5} torr. First, Ar ion bombardment was employed to remove impurities and catalyst particles, and to enhance the doping by creating defect sites on the CNT. Then, oxygen and nitrogen were introduced into the vacuum system. During doping, the ion dosage was monitored by detecting the ion current at the substrate. The CNT-FET was characterized every few minutes at room temperature and at the base pressure of the vacuum system. Finally, the environmental stability of the device was examined in air.

To understand the effect of nitrogen gas, first-principles electronic structure calculations were carried out based on density functional theory.[12] Wave functions were expanded in the pseudo-atomic orbital basis set implemented in the OpenMX package. We employed norm-conserving Troullier–Martins pseudopotentials.[13] For the exchange–correlation term, the Ceperley–Alder type local density approximation was employed, and the energy cutoff for real space mesh points was 130 Ry.[14] The semiconducting (8,0) CNT was chosen with a N_2 substitutional impurity. We chose two model structures with periodic boundary conditions. The supercell size in the lateral direction was 20 Å to avoid interactions between the neighboring CNTs, and the sizes in the axial direction were 17.04 and 34.08 Å for high and low doping, respectively. The atomic positions were relaxed until the forces on the atoms were reduced to 0.05 eV/Å. This clearly shows that the band structure and the Fermi level can be modified depending on the doping concentration of substitutional N_2 dimers.

3. RESULTS AND DISCUSSION

Figure 1(a) shows CNT networks and catalyst particles from a CNT-FET with a 10 μm source–drain electrode gap. In a vacuum, the device exhibits *p*-type behavior (Fig. 1(b)) with an on/off ratio of about 10 that indicates the existence of metallic tubes in the channel. After measuring the *I–V* curves, the devices were degassed at 150–200 °C for 30 minutes and characterized again at room temperature under vacuum. Figure 1(c) shows that I_{sd} increased significantly under a positive gate bias, agreeable with *n*-type behavior of degassed CNTs in a vacuum system.[15] Yet, metallic tubes undermine the gate bias effect in our case.

We conducted Ar ion bombardment on the FET at a beam current of 0.13 μA, corresponding to 1.9×10^{12} ions/sec-cm^2. We examined the *I–V* characteristics of the transistor at room temperature at intervals of 5 minutes. Figure 1(d) shows the *I–V* curves obtained after 30 minutes of exposure, which are not different from those acquired at 5 minutes (not shown). After 30 minute exposure, the on/off ratio of the device jumped from 10 to about 1000. The improved on/off ratio is not because of the increase in the on-current at negative bias, but because of the suppression of the off-current at positive gate bias. Therefore, the enhanced device properties may have been responsible for the deterioration of the electrical conductivity of the metallic nanotubes.

Figure 1(e) shows the morphology of CNT networks exposed to Ar ions for 30 minutes. The catalyst particles between the electrodes were clearly removed. This shows that our results were not influenced by impurities. Although some tubes were found to be truncated due to energetic ions (indicated by arrows), the CNTs maintained networks between the electrodes. The generation of defects by low energy Ar ions can be seen using electron energy loss spectroscopy (EELS) (Fig. 1(f)). A π plasmon peak at 5 eV was attributed to unexposed CNTs that disappeared after Ar ion irradiation. In addition, the overall curve slightly shifted toward lower energies. The shift in the π plasmon implies the growth of non-sp^2 carbon contents in the graphene layers.[16] As can be seen in Figure 1(e), Ar ions kicked out catalyst particles, e-beam resist, gas adsorbates, and even host carbon atoms. Nevertheless, since it restored the uni-polarity and range of CNT-FETs observed in air, Ar ion cleaning was employed as a preliminary step for oxygen and nitrogen doping.

To introduce hole carriers to the CNTs, we irradiated a *p*-type CNT-FET with an on/off ratio of about 100 (Fig. 2(a)) at a doping rate of 2×10^{12} ions/cm^2 oxygen ions per second. Figure 2(b) displays the progressive changes of the *I–V* curves measured during the doping. I_{sd} was obtained at a source–drain bias (V_{sd}) of 3 V. The CNT-FET that showed *p*-type behavior initially exhibited a dramatic drop in I_{sd} at a negative gate bias after 3 and 6 minutes, while no substantial change was seen in

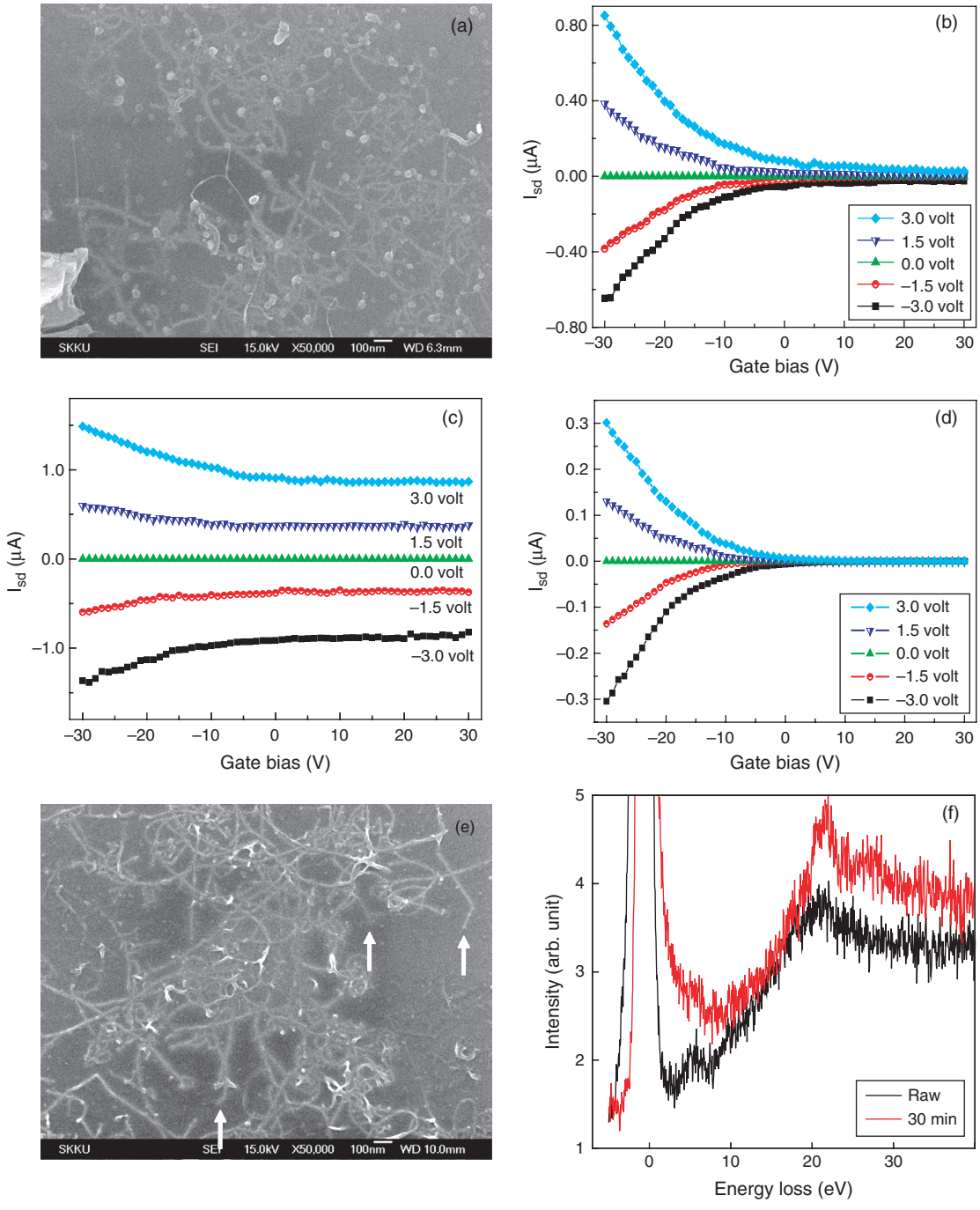

Fig. 1. (a) SEM image of CNT networks between source–drain electrodes. *I–V* curves of CNT-FET obtained (b) in vacuum, (c) after degassing, and (d) after Ar ion bombardment for 30 minutes. (e) SEM image of CNT networks after exposure to Ar ions for 30 minutes. (f) Electron energy loss spectroscopy before and after Ar ion bombardment.

the positive polarity. Together with the current drop, both the slope of the I_{sd} curves and the threshold voltage after 3 and 6 minutes changed substantially compared to those of the pristine sample. In previous study, the slope increase of I_{sd} curves was observed as a CNT-FET was exposed to O_2, whereas no shift of threshold voltage was seen.[15] This implicated undoping of CNTs. Therefore, it was supposed that the gas adsorbates changed the work function of metal such that Fermi level may line up at the top of valance band of CNTs. As a consequence, the Schottky barrier height at the interface became more favorable for hole conduction.[15, 17, 18] This also applies in a present study. The significant decrease of I_{sd} slope may reflect the interfacial barrier change due to incoming molecular oxygen. However, in addition to the slope change, a noticeable increase of threshold voltage concurrently occurred.

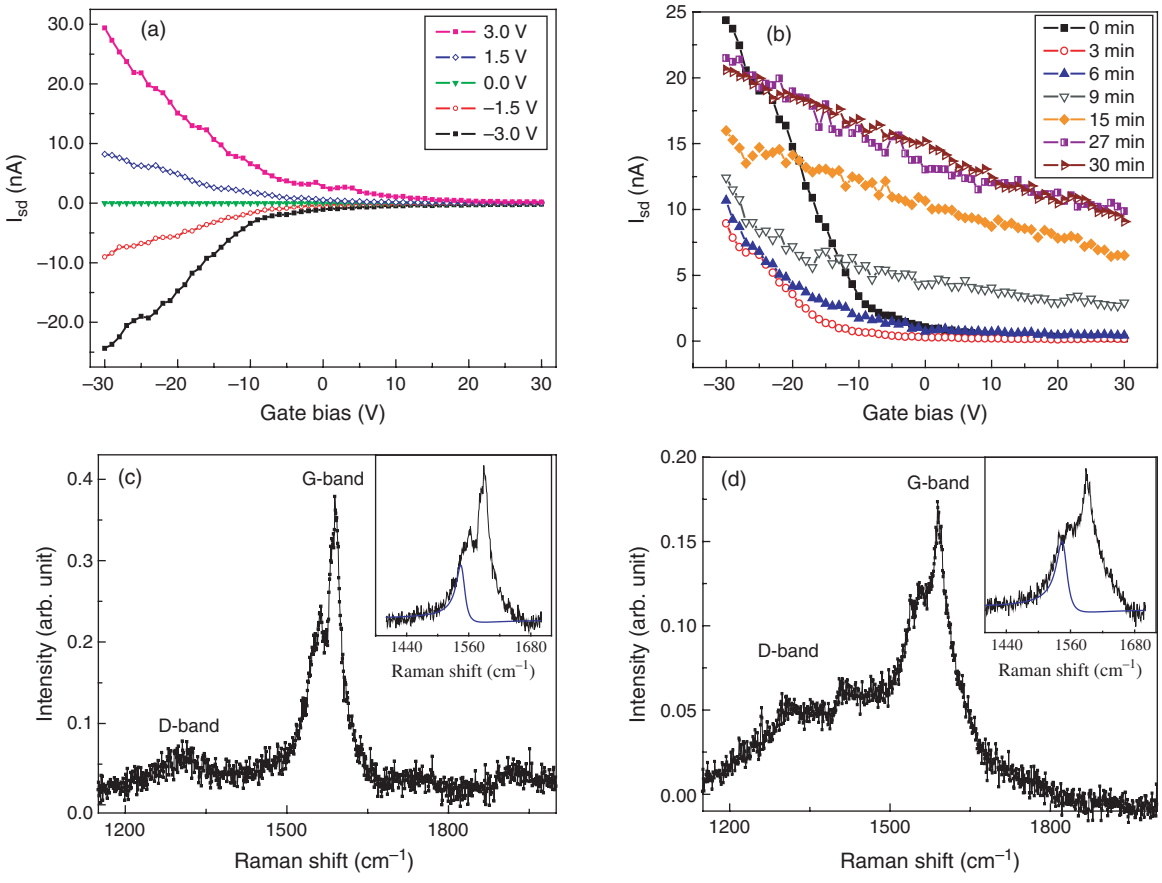

Fig. 2. *I–V* curves measured (a) before, and (b) during oxygen ion bombardment. Raman spectra of CNTs obtained (c) before, and (d) after oxygen ion bombardment. The insets show the G-band with Fano line fit at 1545 cm^{-1}. The wavelength of the laser was 514.4 nm.

Our circumstance is somewhat different from transport study in ambient air. Thermal dissociation of oxygen generated mostly O_2^+ ions. Although oxygen molecules did not dope the CNTs, there were abundant O_2^+ ions that were more chemically reactive and kinetically energetic than molecular oxygen due to the acceleration voltage. Therefore, it is possible that O_2^+ ions would dope the CNTs through adsorption, interstitial, and vacancy defects.[19] Evidence of CNT doping can be seen in Figure 2(b). The increase in threshold voltage after 3 and 6 minutes could be interpreted from the increasing concentration of hole carriers. More evidently, *p*-type behavior disappeared after 9 minutes with considerable I_{sd}, even at zero V_{gs}, indicating heavy doping of the CNTs. Further exposure contributed to a gradual increase in I_{sd}, but the current saturated at 30 minutes (Fig. 2(b)). These results led us to conclude that at low oxygen dosages, the variation in Schottky barrier height caused by O_2^+ ions and/or O_2 dominated the transport properties, whereas at higher dosages, the bulk doping by O_2^+ ions overwhelmed the band-bending at the CNT-metal junction.

After exposing the CNT-FET to oxygen ions, the CNT networks between the source and drain were characterized using Raman spectra. Figures 2(c) and (d) present the D- and G-bands of the CNT networks before and after doping. The G-band near 1600 cm^{-1} comprised six peaks: four from semiconducting tubes, and two from metallic tubes.[20] The peak at 1545 cm^{-1} was designated as a Fano line, which has an intensity associated with the number of metallic tubes in the ensemble. The G-band near 1600 cm^{-1} (Fig. 2(c)) became broader after oxygen doping (Fig. 2(d)). A comparative study of the underlying area of the Fano line at 1545 cm^{-1} in the G-band between the insets of 2(c) and (d) revealed an increase of 5% after oxygen ion bombardment. This indicates that the metallicity of the CNT networks was enhanced by oxygen doping, which is consistent with the metallic behaviors seen in the *I–V* curves in Figure 2(b). It is also important to note that oxygen exposure increased the intensity of the D-band at 1333 cm^{-1} (Fig. 2(d)) and gave rise to a new peak at 1411 cm^{-1} which was composed of sp^2 and sp^3 carbon structures.[21] When we brought the FET into air, the *I–V* curves showed no noticeable changes in device performance.

Following Ar ion cleaning, nitrogen gas was utilized as an *n*-doping agent. The dosage of N_2^+ ion was about 1.9×10^{12} ions/sec-cm^2. Figure 3(a) shows the I_{sd} of a CNT-FET at a V_{sd} of 3 V as a function of exposure time. The FET showed an on/off ratio of about 20 before N_2 ion bombardment. An exposure for 5 minutes resulted in a slight

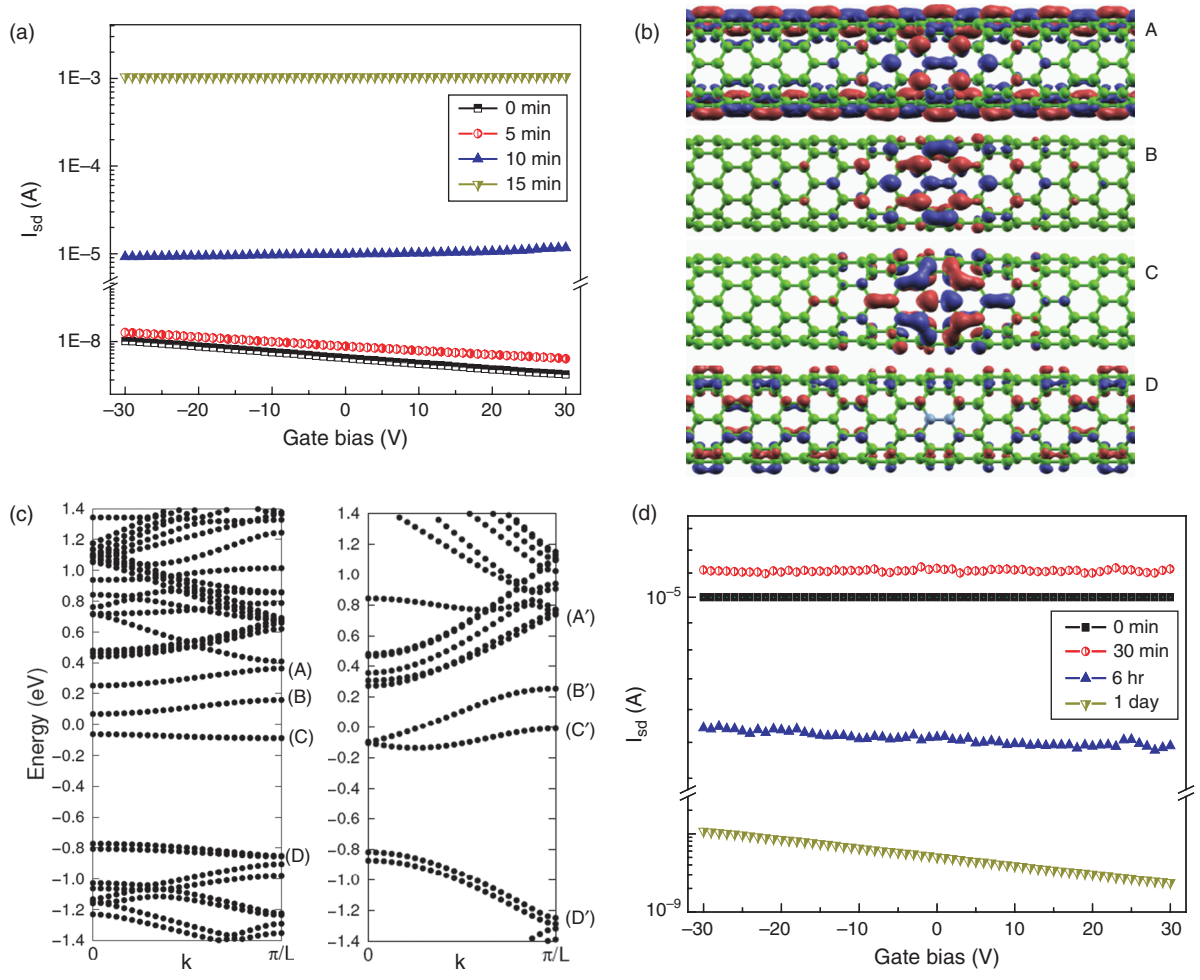

Fig. 3. *I–V* characteristics measured after nitrogen ion bombardment in (a) a vacuum. (b) Wave functions of the N_2-doped (8,0) CNT, and (c) associated band structures at a low dosage (left panel) and a high dosage (right panel). The Fermi level was set to zero. (d) *I–V* characteristics measured in air after nitrogen ion bombardment.

increase in I_{sd}, although the increase was more noticeable at a positive gate bias. It may not be clear whether the uneven increase of I_{sd} can signify possible *n*-type doping by nitrogen gases because of the low on/off ratio of the CNT-FET. However, following exposures of 10 and 15 minutes, it became more obvious that an increased N_2^+ ion dosage endowed the CNTs with stronger metallicity. As a consequence, I_{sd} grew 100,000 times to a few mA after 15 minutes of exposure. Together with an immense current increase, more noticeable growth of I_{sd} at positive gate bias leads us to conclude that N_2^+ ions doped CNT with *n*-type carriers, which is not be agreeable with the case of ammonia.[22]

Using first-principles calculations, we investigated the electronic structure of an N_2-doped (8,0) CNT. For the calculation, we choose two model structures with the periodicities of 17.04 Å (a heavily-doped case) and 34.08 Å (a lightly-doped case) in the axial direction. By the geometry optimization, the N–N bond length becomes 1.50 Å. Figure 3(b) shows the wave functions of an N_2-doped (8,0) CNT. States A and D are the conduction band minimum and the valence band maximum, respectively. States B and C are localized N_2 defect states within the band gap. In Figure 3(c), the lightly-doped CNT exhibits the upshift of the Fermi level by ∼0.3 eV (left panel) and the *n*-type behavior. Here, the two flat bands (localized states) come from substitutional N_2 defect states. This could explain the larger increase of I_{sd} at positive gate in Figure 3(a). At a high doping rate, the CNT exhibited metallic properties due to the overlap of the wave function of the N_2 impurity, which produces two new dispersive bands (States B′ and C′) near the Fermi level (right panel of Fig. 3(c)). The metallic property of CNTs after 10 minute exposure in Figure 2(a) can be appreciated from impurity conduction band by substitutional N_2 dimers.

After doping, the device was brought into air for the stability test, and was characterized at the same V_{sd}. As seen in Figure 3(d), our transistor failed to preserve the large current gain in air. After 24 hours, I_{sd} returned to its level before nitrogen doping. This is probably due to the ambient oxygen and water in air that take up charges from

the CNTs. It also indicates the weak binding of N_2^+ ions on the CNT surface.

4. CONCLUSIONS

In this study, we created defects using Ar ions and implanted CNTs with oxygen and nitrogen ions at a low acceleration voltage. At low dosages, oxygen ions affected the I–V characteristics of the CNT-FET by substantially changing the threshold voltage and slope of I_{sd}. However, at high dosages, the CNT-FET exhibited metallic behaviors. Under nitrogen ion irradiation, we did not observe electron doping of the CNTs at low dosages, but saw a significant increase in I_{sd} of five orders of magnitude at high dosages. Our theoretical calculations showed that the immense increase in I_{sd} was due to the impurity conduction band from substitutional N_2 dimers. Our results showed that oxygen and nitrogen doping affected the increase in the electrical conductivity of the CNT network by removing metal-semiconductor barriers.

Acknowledgments: This work was financially supported by the MOE through the STAR faculty project, by the MOST through the CNNC at SKKU, and by KETI under grant No. 10029846-2007-01. This research was also supported by WCU (World Class University) program under grant No. R31-2008-000-10029-0.

References and Notes

1. T. Durkop, S. A. Getty, E. Cobas, and M. S. Furher, *Nano Lett.* 4, 35 (**2004**).
2. Z. Yao, C. L. Kane, and C. Dekker, *Phys. Rev. Lett.* 84, 2941 (**2000**).
3. S. J. Wind, J. Appenzeller, R. Martel, V. Derycke, and P. Avouris, *Appl. Phys. Lett.* 80, 3817 (**2000**).
4. S. M. Bachilo, M. S. Strano, C. Kittrell, R. H. Hauge, R. E. Smalley, and R. B. Weisman, *Science* 298, 2361 (**2002**).
5. R. Martel, V. Derycke, C. Lavoie, J. Appenzeller, K. K. Chan, J. Tersoff, and P. Avouris, *Phys. Rev. Lett.* 87, 256805 (**2001**).
6. C. Zhou, J. Kong, E. Yenilmez, and H. Dai, *Science* 290, 1552 (**2000**).
7. W. J. Yu, S. Y. Jeong, K. K. Kim, B. R. Kang, D. J. Bae, M. Lee, S. Hong, S. P. Gaunkar, D. Pribat, D. Perello, M. Yun, J. Y. Choi, and Y. H. Lee, *New J. Phys.* 10, 113013 (**2008**).
8. Y. Nosho, Y. Ohno, S. Kishimoto, and T. Mizutani, *Appl. Phys. Lett.* 86, 073105 (**2005**).
9. H.-Z. Geng, K. K. Kim, C. Song, N. T. Xuyen, S. M. Kim, K. A. Park, D. S. Lee, K. H. An, Y. S. Lee, Y. Chang, Y. J. Lee, J. Y. Choi, and Y. H. Lee, *J. Mater. Chem.* 18, 1261 (**2008**).
10. Q. Cao, S.-H. Hur, Z.-T. Zhu, Y. G. Sun, C.-J. Wang, M. A. Meitl, M. Shim, and J. A. Rogers, *Adv. Mater.* 18, 304 (**2006**).
11. Y. Min, E. J. Bae, I. P. Asanov, U. J. Kim, and W. Park, *Nanotechnol.* 18, 285601 (**2007**).
12. W. Kohn and L. J. Sham, *Phys. Rev.* 140, A1133 (**1965**).
13. N. Troullier and J. L. Martins, *Phys. Rev. B* 43, 1993 (**1991**).
14. D. M. Ceperley and B. J. Alder, *Phys. Rev. Lett.* 45, 566 (**1980**).
15. V. Derycke, R. Metal, J, Appenzeller, and Ph. Avouris, *Appl. Phys. Lett.* 80, 2773 (**2002**)
16. P. M. Ajayan, S. Iijima, and T. Ichihashi, *Phys. Rev. B* 47, 6859 (**1993**).
17. D. Kang, N. Park, J. Ko, E. Bae, and W. Park, *Nanotechnol.* 16, 1048 (**2005**).
18. R. Martel, V. Derycke, C. Lavoie, J. Appenzeller, K. Chan, J. Tersoff, and Ph. Avouris, *Phys. Rev. Lett.* 87, 256805 (**2001**).
19. T. Kamimura, K. Yamamoto, T. Kawai, and K. Matsumoto, *Jpn. J. Appl. Phys.* 44, 8237 (**2005**).
20. S. D. M. Brown, A. Jorio, P. Corio, M. S. Dresselhause, G. Dresselhaus, R. Saito, and K Kniepp, *Phys. Rev. B* 63, 155414 (**2001**).
21. D. S. Knight and W. B. White, *J. Mater. Res.* 4, 385 (**1989**).
22. Y. S. Min, E. J. Bae, U. J. Kim, E. H. Lee, N. Park, C. S. Hwang, and W. Park, *Appl. Phys. Lett.* 93, 043113 (**2008**).

Received: 2 February 2009. Revised/Accepted: 13 March 2009.